Solution of the time-dependent Schrödinger equation with absorbing boundary conditions*

Chen Zhidong(陈志东), Zhang Jinyu(张进宇)†, and Yu Zhiping(余志平)†

(Institute of Microelectronics, Tsinghua University, Beijing 100084, China)

Abstract: The performances of absorbing boundary conditions (ABCs) in four widely used finite difference time domain (FDTD) methods, i.e. explicit, implicit, explicit staggered-time, and Chebyshev methods, for solving the time-dependent Schrödinger equation are assessed and compared. The computation efficiency for each approach is also evaluated. A typical evolution problem of a single Gaussian wave packet is chosen to demonstrate the performances of the four methods combined with ABCs. It is found that ABCs perfectly eliminate reflection in implicit and explicit staggered-time methods. However, small reflection still exists in explicit and Chebyshev methods even though ABCs are applied.

Key words: finite difference time domain method; absorbing boundary condition; time-dependent Schrödinger equation

DOI: 10.1088/1674-4926/30/1/012001 **PACC:** 0340K

1. Introduction

The investigation of time-dependent quantum transport in nano devices is drawing a lot of attention[1−3]. The work on time-dependent transport enables researchers to study the transient, AC and RF characteristics of nano devices, e.g., carbon nanotubes (CNT) used as interconnects in integrated circuits. The Schrödinger equation is solved in a device simulation of time-dependent transport. An analytical solution of the Schrödinger equation is hard to find, making the numerical solution the only option. The finite-difference time-domain (FDTD) method is widely used for numerically solving the Schrödinger equation. Numerical device simulation of quantum transport involves the integration in energy space of carriers. Usually hundreds of discrete energy levels are needed for the integration. The simulation is thus very time-consuming. Furthermore, the time step required for FDTD is restricted by the requirement of stability and accuracy. Hence a fast yet accurate algorithm is badly sought by researchers. On the other hand, in device simulation, a natural domain for the problem is infinitely large and thus the boundary conditions have to be specified at infinity. This is obviously not preferred as a finite problem domain is much easier to be handled. An ABC is a convenient way of transforming an infinite domain to a finite one as it does not affect the solution in the interior domain concerned[4].

Many different techniques have been proposed in the implementation of FDTD. These methods, however, are usually designed at their origin to handle the reflecting boundary condition instead. In this paper, we systematically evaluate four such methods, i.e. explicit[5], implicit[5], explicit staggered-time[6], and one-step Chebyshev methods[7], to compare their performances with ABCs being applied. The explicit method is well known to be only conditionally stable[8], although it is easy to implement. The implicit (or Crank-Nicolson) method, on the other hand, is unconditionally stable but is much slower because a set of linear equations is solved at each moment. The explicit staggered-time algorithm was proposed in 1991[6] to improve the stability of the explicit method. Unlike other methods, it treats the real and imaginary components of the wave function separately at staggered moments. The explicit, implicit and explicit staggered methods are second order accurate in time step Δt[7,8]. Another solution method, the one-step Chebyshev method, is also unconditionally stable and its error could be very small, almost to machine precision[9].

A comparison of several methods, including the explicit and Chebyshev methods, for solving the time-dependent Schrödinger equation was conducted in 1991[8]. However, a reflecting boundary condition is used there. In Ref.[4], the ABC of different orders is discussed in detail. However, the algorithm in Ref.[4] is based on an implicit difference scheme. The performances of ABCs in explicit and Chebyshev methods have not been discussed before. Besides, although there are many papers on ABCs[10,11], they are about how to design an efficient ABC; little is given on how to implement it in explicit staggered method and a Chebyshev method. In this paper, we describe in detail how to incorporate an ABC developed in Ref.[4] with all of the above four methods. The performances of the ABCs in these methods are also discussed.

2. Methodologies

The time-dependent Schrödinger equation in one dimension is given as

$$\mathrm{i}\hbar\frac{\partial\psi(x,t)}{\partial t}=-\frac{\hbar^2}{2m}\frac{\partial^2\psi(x,t)}{\partial x^2}+V(x)\psi(x,t), \qquad (1)$$

* Project supported by the State Key Development Program for Basic Research of China (No. 2006CB932404).

† Corresponding author. Email: zhangjinyu@tsinghua.edu.cn; yuzhip@tsinghua.edu.cn

Received 28 February 2008, revised manuscript received 4 September 2008

where $\psi(x,t)$ is the wave function, $V(x)$ is the potential energy distribution and is assumed to be time-independent in our study, m is the electron mass, and $\hbar$ is the reduced Plank constant.

The second order ABC in Ref.[4], which is based on group velocity, is applied as the boundary conditions. The dispersion relation derived from the Schrödinger equation (1) is

$$\hbar^2 k^2 = 2m\left(\hbar\omega - V\right). \tag{2}$$

The group velocity of a wave traveling towards the right is then

$$v = \frac{\partial\omega}{\partial k} = \frac{\hbar k}{m}. \tag{3}$$

Using the correspondence between k and partial derivative in x, i.e., $k \to -\mathrm{i}\dfrac{\partial}{\partial x}$, the differential form of Eq.(3) is obtained as

$$\left(\mathrm{i}\frac{\partial}{\partial x} + \frac{mv}{\hbar}\right)\psi = 0. \tag{4}$$

If Equation (4) is satisfied at the right boundary, a wave traveling towards the right with group velocity v would be absorbed completely. However, in general, a wave is composed of more than one component with different group velocities. Thus a higher order boundary condition is required. The second order form of Eq.(4) is:

$$\left(\mathrm{i}\frac{\partial}{\partial x} + \frac{mv_1}{\hbar}\right)\left(\mathrm{i}\frac{\partial}{\partial x} + \frac{mv_2}{\hbar}\right)\psi = 0, \tag{5}$$

where $v_{1,2}$ are the group velocities of the traveling wave. For a wave traveling towards the left, $v_{1,2}$ are substituted by $-v_{1,2}$ in Eq.(5). With Eqs.(5) and (2), the wave functions at the left and right boundaries are determined by

$$\pm\mathrm{i}\hbar\frac{\partial\psi}{\partial x} - \mathrm{i}\hbar c_1\frac{\partial\psi}{\partial t} + \left(c_1 V - c_2\right)\psi = 0, \tag{6}$$

where $c_1 = 2/(v_1 + v_2), c_2 = mv_1v_2/(v_1 + v_2)$. The positive sign in the first term of Eq.(6) corresponds to the left boundary, while the negative sign corresponds to the right boundary. If $v_1 \neq v_2$, two different components of the wave with group velocities v_1 and v_2 will be absorbed; if $v_1 = v_2$, the component of the wave with group velocity v_1 (or v_2) will be absorbed to the second order.

2.1. Explicit method

The explicit second order difference scheme is applied to solve Eq.(1) numerically. Central difference approximation to both spatial and temporal derivatives is applied for the consideration of conserving time reversal symmetry[8]. The discretized form of Eq.(1) is

$$\mathrm{i}\hbar\frac{\psi_j^{n+1} - \psi_j^{n-1}}{2\Delta t} = -\frac{\hbar^2}{2m}\frac{\psi_{j-1}^n - 2\psi_j^n + \psi_{j+1}^n}{\Delta x^2} + V_j\psi_j^n, \tag{7}$$

where the subscript $j \in [1, N]$ denotes the jth spatial grid and the superscript n denotes the nth temporal grid. N is the total number of spatial grids. Δx is the interval between two adjacent spatial grids and Δt is the time step. Such a scheme is stable only if [8,12]

$$\Delta t \leqslant \frac{\hbar}{\dfrac{2\hbar^2}{m\Delta x^2} + \max\left(|V|\right)}. \tag{8}$$

Wave functions in interior spatial grids are calculated using Eq.(7), whereas those at boundary grids are calculated using Eq.(6). The following implicit difference approximations[4]

$$\begin{aligned}
\psi\left(x,t\right) &= \frac{1}{4}\left(\psi_{j+1}^{n+1} + \psi_j^{n+1} + \psi_{j+1}^n + \psi_j^n\right)\\
\frac{\partial\psi\left(x,t\right)}{\partial x} &= \frac{1}{2\Delta x}\left(\psi_{j+1}^{n+1} - \psi_j^{n+1} + \psi_{j+1}^n - \psi_j^n\right)\\
\frac{\partial\psi\left(x,t\right)}{\partial t} &= \frac{1}{2\Delta t}\left(\psi_{j+1}^{n+1} + \psi_j^{n+1} - \psi_{j+1}^n - \psi_j^n\right),
\end{aligned} \tag{9}$$

are applied to Eq.(6) at the left ($j = 1$) and right ($j = N - 1$) boundaries. It is obvious from Eq.(9) that the wave functions $\psi_{1,N}^{n+1}$ are determined by $\psi_{1,N}^n$ as well as $\psi_{2,N-1}^n$ and $\psi_{2,N-1}^{n+1}$.

2.2. Implicit method

The implicit difference scheme is obtained by averaging the explicit forward difference scheme at the nth moment and the backward difference scheme at the $(n + 1)$th moment, and could be easily derived as

$$\begin{aligned}
&\psi_{j+1}^{n+1} + \left(\alpha - 2 - \beta V_j\right)\psi_j^{n+1} + \psi_{j-1}^{n+1}\\
&\quad = -\psi_{j+1}^n + \left(\alpha + 2 + \beta V_j\right)\psi_j^n - \psi_{j-1}^n,
\end{aligned} \tag{10}$$

where $\alpha = \mathrm{i}\frac{4m\Delta x^2}{\hbar\Delta t}, \beta = \frac{2m\Delta x^2}{\hbar^2}$. The implicit scheme is also referred to as the Crank-Nicolson scheme. The implicit method is unconditionally stable and is accurate to the second order in time step Δt[5]. However, Equation (10) is a tridiagonal set of linear equations and must be solved at each moment. Although there are many specialized techniques for solving tridiagonal systems that can reduce the computational cost, the expense of the implicit method is still large. To update wave functions at the boundaries at each moment, Equation (6) with the difference approximations shown in Eq.(9) is solved, as has been done in the explicit method.

2.3. Explicit staggered method

The explicit staggered method was first proposed in 1991 by Visscher[6]. Since then, it has become a popular algorithm because it preserves the advantages of the explicit method, i.e., it is fast and easy for implementing, and yet it improves the stability compared to the explicit method.

In the explicit and implicit methods described above, the real and imaginary components of the wave function are obtained at the same moment; whereas in the explicit staggered method, they are treated separately at staggered moments. Rewrite the wave function as $\psi\left(x,t\right) = \psi_{\mathrm{R}}\left(x,t\right) + \mathrm{i}\psi_{\mathrm{I}}\left(x,t\right)$, where the subscripts R and I denote the real and imaginary components, respectively. The Schrödinger equation (1) is also rewritten as two coupled partial differential equations as

$$\hbar\frac{\partial\psi_{\mathrm{R}}}{\partial t} = -\frac{\hbar^2}{2m}\frac{\partial^2\psi_{\mathrm{I}}}{\partial x^2} + V\psi_{\mathrm{I}}, \tag{11}$$

$$\hbar\frac{\partial\psi_{\mathrm{I}}}{\partial t} = +\frac{\hbar^2}{2m}\frac{\partial^2\psi_{\mathrm{R}}}{\partial x^2} - V\psi_{\mathrm{R}}. \tag{12}$$

Define the real component ψ_{R} at $0, \Delta t, 2\Delta t, \cdots$ and imaginary component ψ_{I} at $\frac{1}{2}\Delta t, \frac{3}{2}\Delta t, \cdots$. Equations (11) and (12) are therefore discretized as

$$\psi_{\mathrm{R}j}^{n+1} = \psi_{\mathrm{R}j}^{n} - \frac{\hbar\Delta t}{2m\Delta x^2}\left(\psi_{\mathrm{I}j-1}^{n+\frac{1}{2}} - 2\psi_{\mathrm{I}j}^{n+\frac{1}{2}} + \psi_{\mathrm{I}j+1}^{n+\frac{1}{2}}\right) + \frac{\Delta t}{\hbar}V_j\psi_{\mathrm{I}j}^{n+\frac{1}{2}} \tag{13}$$

$$\psi_{\mathrm{I}j}^{n+\frac{1}{2}} = \psi_{\mathrm{I}j}^{n-\frac{1}{2}} + \frac{\hbar\Delta t}{2m\Delta x^2}\left(\psi_{\mathrm{R}j-1}^{n} - 2\psi_{\mathrm{R}j}^{n} + \psi_{\mathrm{R}j+1}^{n}\right) - \frac{\Delta t}{\hbar}V_j\psi_{\mathrm{R}j}^{n}. \tag{14}$$

Equations (13) and (14) are solved in an iterative way. First $\psi_{\mathrm{I}}^{n+\frac{1}{2}}$ is calculated using Eq. (14) with the knowledge of $\psi_{\mathrm{I}}^{n-\frac{1}{2}}$ and ψ_{R}^{n}. Then ψ_{R}^{n+1} is obtained using Eq. (13) with the knowledge of ψ_{R}^{n} and newly calculated $\psi_{\mathrm{I}}^{n+\frac{1}{2}}$.

The explicit staggered scheme is stable only if [12]

$$\Delta t \leqslant \frac{\hbar}{\dfrac{\hbar^2}{m\Delta x^2} + \max\left(|V|\right)}. \tag{15}$$

By comparing Eq.(15) with Eq.(8), it is evident that with the same spatial grids and when the potential is zero, the critical time step, i.e., under which the scheme is stable, of the explicit staggered method is twice that of the explicit method. To apply the ABC at the boundary grids, rewrite Eq.(6) as two coupled equations:

$$\pm\hbar\frac{\partial\psi_{\mathrm{R}}}{\partial x} - \hbar c_1\frac{\partial\psi_{\mathrm{R}}}{\partial \mathrm{t}} + \left(c_1 V - c_2\right)\psi_{\mathrm{I}} = 0, \tag{16}$$

$$\mp\hbar\frac{\partial\psi_{\mathrm{I}}}{\partial x} + \hbar c_1\frac{\partial\psi_{\mathrm{I}}}{\partial t} + \left(c_1 V - c_2\right)\psi_{\mathrm{R}} = 0. \tag{17}$$

The upper signs correspond to the left boundary and the lower signs correspond to the right boundary. Equations (16) and (17) are discretized by applying Eq.(9) except for

$$\psi_{\mathrm{I}}(x,t) = \tfrac{1}{2}\left(\psi_{\mathrm{I}j}^{n+\frac{1}{2}} + \psi_{\mathrm{I}j+1}^{n+\frac{1}{2}}\right) \text{ and } \psi_{\mathrm{R}}(x,t) = \tfrac{1}{2}\left(\psi_{\mathrm{R}j}^{n} + \psi_{\mathrm{R}j+1}^{n}\right),$$
$$j = 1 \text{ or } N-1.$$

The boundary conditions for real and imaginary components are also treated at different moments. The numerical procedure of the explicit staggered method is as follows. First, imaginary components of wave functions at the interior grids are calculated using Eq.(14), and then those at the boundary grids are calculated using Eq.(17). Next real components of wave functions at the interior grids are calculated using Eq.(13), and then those at the boundary grids are calculated using Eq.(16).

2.4. One-step Chebyshev method

The application of the Chebyshev method can be traced back to 1984[7]. Compared to other methods, the Chebyshev method can use very big time steps; sometimes a single time step completes the calculation. Rewrite the time-dependent Schrödinger equation (1) as

$$\mathrm{i}\hbar\frac{\partial\psi(x,t)}{\partial t} = H\psi(x,t), \tag{18}$$

where $H = -\dfrac{\hbar^2}{2m}\dfrac{\partial^2}{\partial x^2} + V$. A general solution of Eq.(18) is of the form:

$$\psi(t+\Delta t) = \exp\left(-\frac{\mathrm{i}}{\hbar}H\,\Delta t\right)\psi(t). \tag{19}$$

The main idea of the Chebyshev method is to use a Chebyshev polynomial expansion to approximate the evolution operator $\exp\left(-\dfrac{\mathrm{i}}{\hbar}H\Delta t\right)$. The reason that one does not use Taylor expansion is that the Taylor expansion would lead to the explicit scheme described above[7].

Note that the Hamiltonian matrix H is symmetric. We start by normalizing H. Let $\lambda_{\max}$ be the largest eigenvalue in magnitude and $\|H\|_1$ be 1−norm of H. Using the fact that $\lambda_{\max} \leqslant \|H\|_1$, the eigenvalues of the normalized matrix $B = -\dfrac{H}{\|H\|_1}$ are found to lie in $[-1,1]$, which makes the Chebyshev method unconditionally stable. Since B is also symmetric, it is diagonalizable, i.e., it has a complete set of orthonormal eigenvectors. Let $z = \dfrac{\|H\|_1}{\hbar}\Delta t$, then $\exp\left(-\dfrac{\mathrm{i}}{\hbar}H\Delta t\right) = \exp\left(\mathrm{i}zB\right)$. By expanding the right hand side of Eq.(19) with Chebyshev polynomials[7],we have

$$\psi(t+\Delta t) = \mathrm{e}^{\mathrm{i}zB}\psi(t) = \left[J_0(z) + 2\sum_{k=1}^{\infty}\mathrm{i}^k J_k(z)\,T_k(B)\right]\psi(t), \tag{20}$$

where $J_k(z)$ is the Bessel function of the first kind of order k, and $T_k(B)$ is a matrix-valued Chebyshev polynomial defined by the following recursion relations:

$$T_0(B)\psi(t) = \psi(t),\ T_1(B)\psi(t) = B\psi(t)$$

$$T_{k+1}(B)\psi(t) = 2BT_k(B)\psi(t) - T_{k-1}(B)\psi(t),\ k = 1, 2, \cdots$$

In deriving Eq.(20), the fact that H is diagonalizable, i.e., it has a complete set of orthogonal eigenvectors, is implied. In practical use, the summation in Eq.(20) is truncated. It is found that when k is larger than z, $J_k(z)$ vanishes exponentially[7,9]. Thus we truncate the summation in Eq.(20) when $|J_k(z)| \leqslant \varepsilon$, where ε is taken to be 10^{-10}.

Refinement of this method is based on increasing expansion order, rather than by decreasing time steps as the other three methods described above do. Furthermore, the time steps of the Chebyshev method can be extremely big. The main drawback of the Chebyshev method is that during one time step, the potential distribution should be unvaried. With time-dependent potential, its time step is limited by the speed of potential variation. As a result, the efficiency of this method is greatly reduced. However, in device simulation where the Poisson equation is solved accompanying the Schrödinger equation, the variation of potential is much slower than the evolution of wave functions. In other words, during a relatively large time step, the potential could be assumed to be unvaried. Thus the Chebyshev method is still an efficient method. When taking the ABC into account, combining Eq.(6) with Eq.(18) would lead to a new Hamiltonian:

$$\hat{H} = \begin{bmatrix} \frac{c_1V_1 - c_2}{2c_1} - \frac{\mathrm{i}\hbar}{c_1\Delta x} & \frac{c_1V_1 - c_2}{2c_1} + \frac{\mathrm{i}\hbar}{c_1\Delta x} & & & \\ -\frac{\hbar^2}{2m\Delta x^2} & \frac{\hbar^2}{m\Delta x^2} + V_2 & -\frac{\hbar^2}{2m\Delta x^2} & & \\ & \ddots & \ddots & \ddots & \\ & & -\frac{\hbar^2}{2m\Delta x^2} & \frac{\hbar^2}{m\Delta x^2} + V_{N-1} & -\frac{\hbar^2}{2m\Delta x^2} \\ & & & \frac{c_1V_N - c_2}{2c_1} + \frac{\mathrm{i}\hbar}{c_1\Delta x} & \frac{c_1V_N - c_2}{2c_1} - \frac{\mathrm{i}\hbar}{c_1\Delta x} \end{bmatrix}.$$

Note that $\hat{H}$ is now non-symmetric. However, the eigenvectors of the new Hamiltonian $\hat{H}$ are basically still orthogonal. As a result the Chebyshev method still works in this situation.

3. Numerical verification and discussion

Assume that the initial wave function is a single Gaussian distribution given by

$$\psi_j^0 = \exp\left(-\frac{\left(x_j - \xi\right)^2}{2\sigma^2}\right)\exp\left(\mathrm{i}k_0x_j\right),\ j = 1, 2, \cdots, N.$$

Further assume that the potential is zero. A Gaussian distribution is chosen as the initial wave function for the following consideration[4]. Any wave function could be expressed in terms of Fourier modes, which are essentially plane waves. Therefore, since the carrier wave of a Gaussian distribution is a plane wave, if the ABC is well behaved for various plane waves with different frequencies, it is expected to be well behaved for any initial wave function whose Fourier modes are dominated at these frequencies.

In our numerical simulation, $\hbar = 1, m = 0.5$. The simulation domain is chosen to be $x \in [-20, 20]$ with 600 spatial grids. Other parameters of the initial Gaussian wave packet are $\xi = -15, \sigma = 2, k_0 = 2.5$. The exact solution is used as a benchmark[13].

The computation times of the four methods described in Section 2 are compared first. The critical time steps of the explicit method Δt_{c1} and the explicit staggered method Δt_{c2} are determined by Eqs.(8) and (15), respectively. Numerical experiments show that the explicit and explicit staggered methods with their respective critical time steps are not always stable. To prevent the instability problem from happening, we choose $\Delta t = 0.3\Delta t_{c1}$ for the explicit method and $\Delta t = 0.3\Delta t_{c2}$ for the explicit staggered method. The computation times of the four methods in which the Gaussian wave packet evolves from $t = 0$ to $t = 0.6$ are listed in Table 1. More time is consumed in the explicit method than in the explicit staggered and Chebyshev methods. The Chebyshev method is unconditionally stable even with such a big time step, and it is more efficient than the explicit method. The implicit method with $\Delta t = \Delta t_{c2}$ is the most time-consuming. As the implicit method is also unconditionally stable, a bigger time step could be applied, e.g., $\Delta t = 5\Delta t_{c2}$, without causing a stability problem. Therefore its computational time is significantly reduced.

Table 1. Comparison of computation time from t =0 to t =0.6.

Method	Computation time (s)
Explicit $\Delta t = 0.3\Delta t_{c1}$	4.04
Explicit staggered $\Delta t = 0.3\Delta t_{c2}$	2.06
Implicit $\Delta t = \Delta t_{c2}$	6.52
$\Delta t = 5\Delta t_{c2}$	1.28
Chebyshev $\Delta t = 0.6 \approx 270\Delta t_{c2}$	1.93

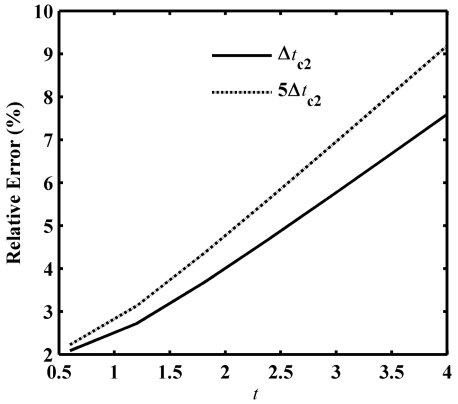

Fig.1. Relative errors of the implicit method with different time steps.

However, its error, on the other hand, increases as the time step increases, due to its second order accuracy in Δt. Relative errors of the implicit method with respect to the exact solution are plotted in Fig.1. Two different time steps, i.e., Δt_{c2} and $5\Delta t_{c2}$, are demonstrated here. With a bigger time step, the error is larger and grows faster. As a result, when using the implicit method, a reasonable time step needs to be carefully chosen because of the tradeoff between accuracy and efficiency.

Next, we examine the performances of the four methods combined with the ABCs using a parameter r[4] defined as

$$r = \frac{\sum_j \left|\psi_j^n\right|^2}{\sum_j \left|\psi_j^0\right|^2}.$$

With perfect ABCs, when the wave passes through the boundaries, r gradually vanishes; whereas with reflecting boundary conditions where the wave is reflected from the boundaries, r is non-vanishing.

r computed from the four methods as a function of time is illustrated in Fig.2. The time step of the implicit method is

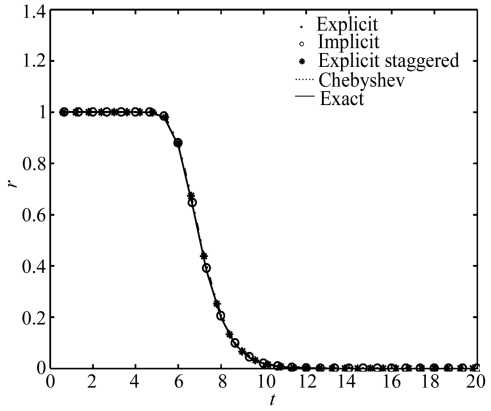

Fig.2. r versus time for different methods. r from the exact solution is also plotted as a benchmark.

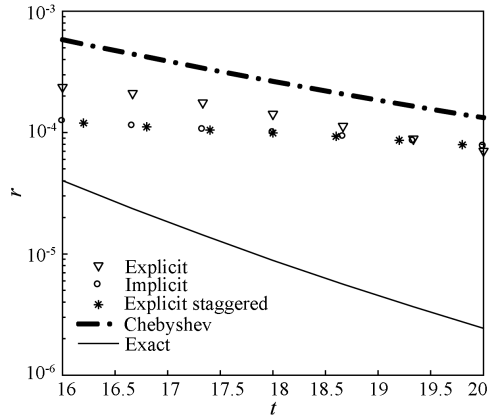

Fig.3. r versus time for different methods after most of the wave has passed through the boundary.

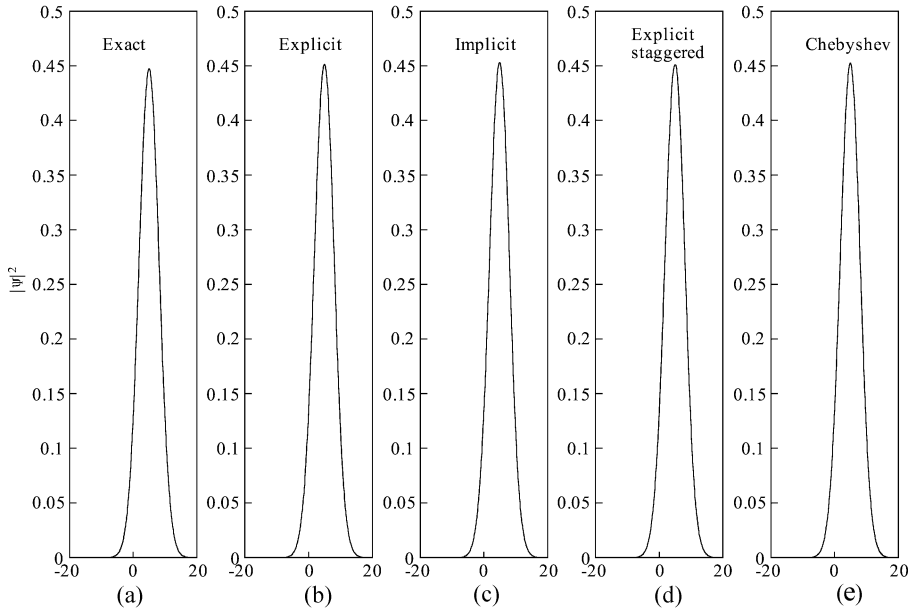

Fig.4. Squares of the amplitudes of the right-moving wave in the four methods as well as in the exact solution at $t = 4$, i.e., before the wave impinges on the right boundary.

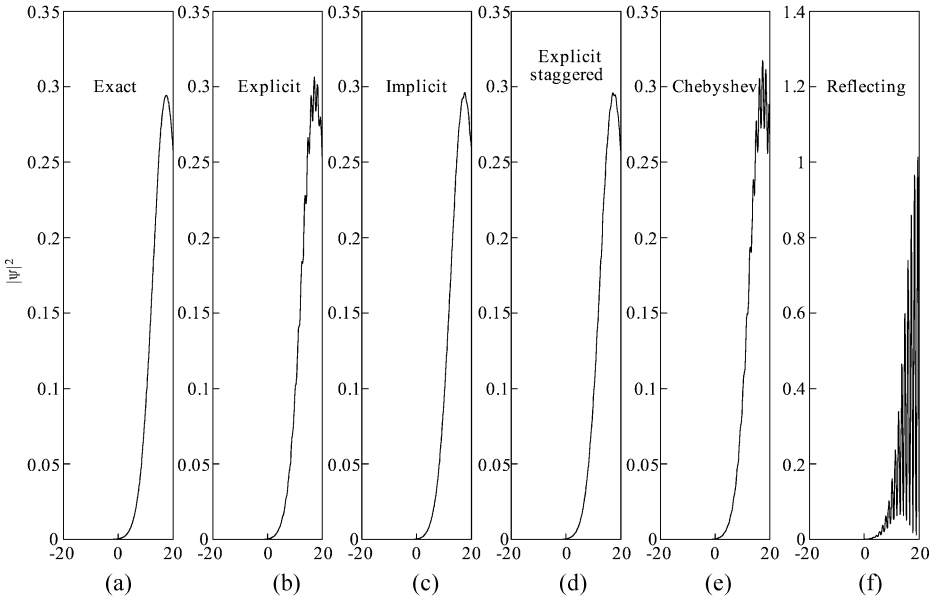

Fig.5. (a)–(e) Squares of the amplitudes of the right-moving wave in the four methods as well as in the exact solution at $t = 6.5$, i.e., when part of the wave has passed through the right boundary; (f) Result with the reflecting boundary condition.

$\Delta t = \Delta t_{c2}$. At the beginning, r equals 1 as the wave is completely in the simulation domain. As soon as the wave impinges on the boundary, it starts to pass through the boundary; in the mean time r begins to decrease. After the entire wave has passed through the boundary, r vanishes. As shown in Fig.2, variations of r from the four methods are in good accord with that from the exact solution. It is thus concluded that the ABC works in the four methods. However, speeds of r decreasing to 0 are a little different within these four methods and the exact solution. Figure 3 shows r versus time after most of the wave has passed through the boundary. It is obvious from Fig.3 that the ABC performs best in the implicit and explicit staggered methods. The performance of the ABC in the Chebyshev method is the worst, i.e., it will cause more reflection from boundaries than the other three methods.

Squares of amplitudes of the right-moving wave calculated from the four methods as well as from the exact solution at $t = 4$ (before the wave impinges on the boundary) and $t = 6.5$ (part of the wave has passed through the boundary) are plotted in Figs.4 and 5, respectively. As shown in Fig.4, before the wave impinges on the right boundary, all of the four methods produce numerically accurate solutions. On the other hand, as plotted in Fig.5, when the wave impinges on the boundary and starts to pass through it, the results computed by the four methods are different. Reflection is perfectly eliminated in the implicit and explicit staggered methods. However, small reflection still exists in the explicit and Chebyshev methods. The wave function computed with reflecting boundary conditions is also plotted in Fig.5 (f) as a comparison. Although applying the implicit difference approximations in Eq.(9) on boundary equation (6) eliminates reflection in the implicit and explicit staggered methods, it does not produce the same good result in the explicit method. Reflection in the Chebyshev method is the most severe among all four methods, as shown in Fig.5 (e). The problem with the Chebyshev method is that it could not reduce reflection by simply using higher order or implicit difference approximation, e.g. Eq.(9), as has been done in the other three methods. Another possible reason for reflection in the Chebyshev method arises from the fact that when taking the ABC into account, the Hamiltonian $\hat{H}$ is not exactly orthogonal. As a result, a minor error may exist in the expansion with Chebyshev polynomials.

In summary, it is evident that to obtain an accurate result which perfectly reproduces the exact solution, the implicit and explicit staggered methods are appropriate choices. For the further consideration of efficiency where a much larger time step is necessitated, the explicit staggered method is unlikely to be feasible in order to avoid stability problem. The implicit method with a reasonably large time step, on the other hand, is suitable for improving computation efficiency while not causing a stability problem.

4. Conclusion

The performances of ABCs in four widely used FDTD methods, i.e., explicit, implicit, explicit staggered and Chebyshev methods, are discussed. The computation efficiency of the four methods is also compared. The explicit and explicit staggered methods are conditionally stable and small time steps are adopted to avoid causing a stability problem. The Chebyshev method is unconditionally stable and efficient compared to the other methods. The implicit method is also unconditionally stable. A reasonable time step needs to be carefully chosen in this method due to the tradeoff between efficiency and accuracy. The ABC performs best in the implicit and explicit staggered methods. Reflection is eliminated in these two methods. Small reflection still exists in the explicit and Chebyshev methods even though the ABC is applied.

References

[1] Chen Yupeng, Ouyang Yijian, Guo Jing, et al. Time-dependent quantum transport and nonquasistatic effects in carbon nanotube transistors. Appl Phys Lett, 2006, 89(20): 203122

[2] Sullivan D, Citrin D S. Time-domain simulation of two electrons in a quantum dot. J Appl Phys, 2001, 89(7): 3841

[3] He Yuhui, Hou Danqiong, Liu Xiaoyan, et al. Time-dependent transport in low-dimensional systems: a numerical solution using the nonequilibrium Green's functions. IEEE Trans Nanotech, 2007, 6(1): 56

[4] Fevens T, Jiang H. Absorbing boundary conditions for the Schrödinger equation. SIAM J Sci Comput, 1999, 21(1): 255

[5] Burden R L, Faires J D. Numerical analysis. 7th ed. Pacific Grove, CA: Brooks/Cole, 2001

[6] Visscher P B. A fast explicit algorithm for the time-dependent Schrödinger equation. Comput Phys, 1991, 5: 596

[7] Tal-Ezer H, Kosloff R. An accurate and efficient scheme for propagating the time dependent Schrödinger equation. J Chem Phys, 1984, 81(9): 3967

[8] Leforestier C, Bisseling R H, Cerjan C, et al. A comparison of different propagation schemes for the time dependent Schrödinger equation. J Comp Phys, 1991, 94(1): 59

[9] De Raedt H, Michielsen K, Kole J S, et al. One-step finite-difference time-domain algorithm to solve the Maxwell equations. Phys Rev E, 2003, 67(5): 056706

[10] Givoli D, Neta B. High-order non-reflecting boundary scheme for time-dependent waves. J Comput Phys, 2003, 186(1): 24

[11] Szeftel J. Design of absorbing boundary conditions for Schrödinger equations in R^d. SIAM J Numer Anal, 2004, 42(4): 1527

[12] Soriano A, Navarro E A, Porti J A, et al. Analysis of the finite difference time domain technique to solve the Schrödinger equation for quantum devices. J Appl Phys, 2004, 95(12): 8011

[13] We use Mathematica to generate this exact solution.